

HST Imaging of the Globular Clusters in the Fornax Cluster: Color and Luminosity Distributions¹

Carl J. Grillmair

SIRTF Science Center, California Institute of Technology, Mail Stop 100-22, Pasadena, California
91125

email: carl@ipac.caltech.edu

Duncan A. Forbes

School of Physics and Astronomy, University of Birmingham, Edgbaston
Birmingham B15 2TT, United Kingdom

email: forbes@star.sr.bham.ac.uk

Jean Brodie

Lick Observatory, University of California, Santa Cruz, California, 95064

email: brodie@ucolick.org

Rebecca Elson

Institute of Astronomy, Madingley Road, Cambridge CB3 0HA, England

email: elson@ast.cam.ac.uk

ABSTRACT

We examine the luminosity and $B - I$ color distribution of globular clusters for three early-type galaxies in the Fornax cluster using imaging data from the Wide Field/Planetary Camera 2 on the *Hubble Space Telescope*. The luminosity functions we derive are in most cases better than 50% complete down to $B = 26.6$. We find that the color distributions of globular clusters in the central region of NGC 1399 and its nearby neighbor NGC 1404 are bimodal and statistically indistinguishable. The metallicity spread, as inferred from the color distributions in these two galaxies, is very similar to that of M 87. NGC 1399's luminosity function is also very similar to that of M 87, and comparing their respective peak magnitudes indicates that the Fornax cluster is at very nearly the same distance from the Local Group as is the Virgo cluster. From this we derive $H_0 = 82 \pm 8 \text{ km s}^{-1} \text{ Mpc}^{-1}$, where the uncertainty reflects only the effects of random errors. The number of unresolved objects we find at a projected distance of 440 kpc from NGC 1399 is consistent with nothing more than compact background galaxies, though the small field of view of the WFPC2 does not allow us to put strong constraints on the number of intergalactic globular clusters. The luminosity function

¹Based on observations with the NASA/ESA Hubble Space Telescope, obtained at the Space Telescope Science Institute, which is operated by AURA, Inc., under NASA contract NAS 5-26555.

of objects detected around NGC 1316 is more nearly exponential than log-normal, and both the color and size distribution of these objects distinguishes them from the clusters surrounding NGC 1399. We suggest that these objects are more akin to old open clusters in the Galaxy than they are to globular clusters in typical early-type galaxies.

Subject headings: galaxies: elliptical and lenticular, galaxies: evolution, galaxies: individual: NGC 1399, galaxies: individual: NGC 1404, galaxies: individual: NGC 1316

1. Introduction.

The characterization of the globular cluster luminosity function (GCLF) remains a high priority as a means to better understand both the formation of globular clusters and the buildup of galaxies. The differences in the breadth and peak position of GCLFs in late-type galaxies in the Local Group and early-type galaxies in other clusters has been known for some time (Harris et al. 1991). Efforts to use GCLFs as distance indicators or tracers of galaxy mergers would clearly benefit from more complete coverage over luminosity and galaxy type. With its $0''.1$ resolution, low sky background, and consequent ability to distinguish very faint point-sources, the *Hubble Space Telescope (HST)* is an ideal platform from which to carry out such a study.

The first surveys of globular clusters in the Fornax cluster were carried out photographically (Dawe & Dickens 1976; Hanes & Harris 1986; Harris & Hanes 1987). Later CCD studies (see Ashman & Zepf 1997 for a list of references) detected bimodal color distributions (Zepf & Ashman 1993) and color gradients (Ostrov, Geisler, & Forte 1993) in the cluster system of NGC 1399. *HST* studies have now confirmed the existence of multi-modal color distributions in several other giant ellipticals (e.g. M 87, Elson & Santiago 1996b; Whitmore et al. 1995; NGC 5846, Forbes et al. 1997a). What follows is the first systematic *HST* investigation of the globular cluster systems in the Fornax cluster. The results should help us to understand how cD galaxies and their large associated globular cluster populations formed (Ashman & Zepf 1992; Forbes, Brodie, & Grillmair 1997b).

One aim of this study is to search for variations in the GC populations among a sample of early-type galaxies in the same cluster. In this paper we examine the globular cluster populations of NGC 1399, NGC 1404, and NGC 1316. In companion papers we study the metallicity and spatial distributions of globular clusters in NGC 1399 and NGC 1404 (Forbes et al. 1998) and examine the globular cluster system of the lower luminosity elliptical NGC 1379 (Elson et al. 1998). NGC 1399 is the cD elliptical at the center of the Fornax cluster and, like M 87, has an extraordinarily large number of globular clusters for its luminosity (see references in Ashman & Zepf 1997). NGC 1404 is an E1 elliptical about half a magnitude fainter and lying only 10 arcminutes from NGC 1399 in projection. Attempts to study its globular cluster system (Hanes & Harris 1986; Richtler et al. 1992) have been complicated by its location within the extended envelope of NGC 1399. NGC 1316 is another giant elliptical in the Fornax cluster, more than a magnitude brighter than NGC

Fig. 1.— Digitized Sky Survey image of the Fornax cluster showing positions and orientations of three of the four WFPC2 pointings discussed in this paper. The NGC 1379 pointing is discussed separately by Elson et al. (1997). The entire field shown here subtends 2° on a side.

1399, with a double-lobed radio source (Fornax A), an X-ray halo, and dust and other irregularities (Schweizer 1980) indicating a recent merger. NGC 1316 is situated more than three degrees away from NGC 1399, clearly dominating its corner of the Fornax cluster, and has been the subject of a recent WFPC1 study by Shaya et al. (1996).

If the high specific frequency of globular clusters around NGC 1399 is to be attributed to tidal stripping or accretion of existing globular clusters in other cluster galaxies (which would be consistent with the kinematic data of Grillmair et al. 1994a and Kissler-Patig et al. 1997b), we might expect mean GC metallicities to be very similar to those of other cluster galaxies. Alternatively, if much of NGC 1399’s globular cluster system formed more recently from enriched gas, its globulars may be overly metal-rich compared to other galaxies of the same magnitude. If new globular clusters are formed in the normal course of mergers (Ashman & Zepf 1992), then we might expect to see a a number of young, metal-rich globulars surrounding NGC 1316.

We describe the observations and their analysis in Section 2. The color distribution of detected globular clusters is discussed in Section 3. We analyze and compare the luminosity functions in Section 4. Section 5 more closely examines the characteristics of objects around NGC 1316, and Section 6 briefly discusses the possibility of intergalactic globular clusters in our sample. We summarize our conclusions in Section 7. The metallicity and spatial distributions of globular clusters in these galaxies and their implications for formation scenarios are discussed by Forbes et al. (1998).

2. Observations and Photometry.

An observing log for program GO #5990 is given in Table 1. While NGC 1379 was observed as an example of a “normal” elliptical, telescope acquisition problems prevented useful F814W data from being taken by the time of writing. The NGC 1379 observations in the F450W filter are discussed by Elson et al. (1998). Field 0338 (F0338) is situated in the cD envelope of NGC 1399, at approximately the same projected distance from NGC 1399 as NGC 1404, but on the opposite side of the galaxy. Field 0336 (F0336) is situated approximately 1.4 degrees south of NGC 1399 in a blank region of sky and serves to measure the surface density of background sources. The relative positions and orientations of these fields are shown in Figure 1. Filters F450W ($\sim B$) and F814W ($\sim I$) were chosen to increase metal sensitivity by about a factor of two over that attainable using $B - V$ (Brodie 1981; Geisler, Lee, & Kim 1996). The images were ADC-corrected, bias-subtracted, and flat-fielded in the course of standard pipeline processing.

Table 1. Observing Log.

Target	RA J2000	Dec	Date	Filter	Exposure Times s	Orientation ^a °
NGC 1399	03 38 29.0	-35 27 00.5	1996 Jun 2	F814W	3 × 600	242.0
NGC 1399			1996 Jun 2	F450W	4 × 1300	242.0
NGC 1379	03 36 03.9	-35 26 26.0	1996 Mar 11	F814W	3 × 0.5	148.3
NGC 1379			1996 Mar 11	F450W	2 × 1300 + 2 × 500 + 1400	148.3
NGC 1404	03 38 51.7	-35 35 36.0	1996 Apr 3	F814W	260 + 600 + 1000	171.8
NGC 1404			1996 Apr 3	F450W	2 × 500 + 2 × 1300 + 1400	171.8
NGC 1316	03 22 41.8	-37 12 29.8	1996 Apr 7	F814W	260 + 600 + 1000	181.3
NGC 1316			1996 Apr 7	F450W	2 × 500 + 2 × 1300 + 1400	181.3
Field 0338	03 37 57.0	-35 21 54.5	1996 Apr 6	F814W	3 × 600	175.3
Field 0338			1996 Apr 6	F450W	4 × 1300	175.3
Field 0336	03 36 02.7	-36 45 54.0	1996 Apr 11	F814W	3 × 600	182.4
Field 0336			1996 Apr 11	F450W	4 × 1300	182.4

Note. —

^aAngle, measured North through East, of the y-axis of the PC chip.

Each set of between 3 and 5 exposures of a given field was split into two pointings offset by $0''.5$ from one another. This corresponds approximately to integer pixel shifts in both the PC ($0''.0455 \text{ pix}^{-1}$) and the WF chips ($0''.0996 \text{ pix}^{-1}$) (the actual shifts are generally within 0.1 pixels of integer values). Aligning and median-combining the images consequently allowed us to eliminate the majority of cosmic rays and hot pixels at the same time. To prevent as much as possible the contamination of the faint end of the GCLF, known warm/hot pixels, charge traps, and bad columns were flagged and subsequently ignored in the median procedure. The distribution of unflagged pixels was further tested for the presence of cosmic ray events before computing the median value from the remaining pixels. The results were found to be cleaner both statistically and visually when compared with the results of such standard cosmic-ray removal procedures as are available, for example, within STSDAS/IRAF.

The PC images of the sample galaxies were analyzed using the VISTA surface-brightness profile-fitting routine SNUC, which fits logarithmically-spaced, concentric ellipses to unmasked portions of the galaxy profile. The resulting model profiles were then subtracted from each image in an effort to flatten the background as much as possible. For the WF chips, similar model surface brightness distributions were generated using both large-scale window-medianing, and convolution with a two-dimensional Gaussian having $\sigma = 1''.0$. Luminosity fluctuations in F0336 and F0338 were found to be on scales sufficiently large that model subtraction was deemed unnecessary.

Source detection and aperture photometry were carried out using DAOPHOT II (Stetson 1987). Owing to the high resolution inherent in these images, overlap of sources was negligible and aperture photometry yielded a slightly narrower color distribution than could be obtained using PSF-fitting photometry. The detection threshold was fixed at three times the rms expected *locally* from photon statistics and readout noise, the former computed by taking into account the subtracted model surface-brightness distributions. Given the degree of undersampling inherent to the WFPC2 detectors, a 3σ detection threshold predictably yielded a substantial number of spurious detections. However, the final photometry table was generated using only those sources which were detected in both passbands and having colors in the range $-1.0 < B - I < 4.0$. Consequently, the number of spurious detections remaining in the final sample (as determined by visual inspection) was found to be negligible.

NGC 1316 is something of a special case in our sample owing to the presence of large amounts of dust obscuration. For this galaxy, we masked large areas of the WFPC2 field of view in which there was visible evidence of dust in F450W. The extent of the dust and the regions we chose to exclude from analysis are shown in Figure 2. The “unobscured” detections attributed to NGC 1316 thus come from approximately the outer halves of each of the WF chips; detections in the PC are not considered in the subsequent analysis owing to the strong likelihood that all detections are obscured and reddened to a significant extent.

Faint background galaxies and bright foreground stars often produced multiple detections along spiral arms or diffraction spikes, and several small regions of each image were masked accordingly.

Fig. 2.— The WFPC2 F450W image of NGC 1316 divided by a model surface-brightness distribution. The demarcation is that beyond which clusters were deemed *not* to be seriously affected by extinction and reddening. Note the interesting, radially-oriented columns of dust in WF4, which suggest Rayleigh-Taylor instabilities or erosion by particles or radiation from the nucleus of the galaxy.

In addition, we disregarded all detections with $m_1 - m_2$ (the difference in magnitude computed for apertures of radius 1 and 2 pixels, respectively) < -0.9 magnitudes (< -1.1 magnitudes for the PC). Visual examination showed that this effectively removed almost all obvious faint galaxies from the sample. A more extensive discussion of the contamination issue is presented by Elson et al. (1998), and as we show presently, the number of background objects in our sample to $B = 26.5$ is $< 2\%$.

At the distance of the Fornax cluster, typical globular clusters are marginally resolved by WFPC2. Treating them as point sources from the standpoint of photometry would therefore underestimate to varying degrees their total luminosities (see Holtzman et al. 1996 for a discussion of this problem). To estimate this shortfall, we convolved an array of King models (King 1966) with WFPC2 PSFs generated using Tiny Tim (Krist 1995) for each globular’s position on the detector. We then sampled these models using WFPC2-sized pixels and a 5×5 grid of pixel-centerings. Each model realization was then compared on a pixel-by-pixel basis with the real data in the NGC 1399 images for $r \leq 3$ pixels to compute χ^2 .

While this procedure yielded a range of best-fit core radii not unlike that found in Galactic globular clusters, it failed sufficiently often that we do not regard the computed core radii as reliable. The reasons for this may include the fact that we did not take into account image dithering and subsequent integer-pixel shifting used to combat hot pixels, as well as inaccuracies in the Tiny Tim model PSFs. However, aperture corrections derived from King model fits with acceptable values of χ^2 agreed very well with those determined empirically for the brightest, most isolated clusters in the field. We therefore adopted mean $0''.5$ aperture corrections to our 2-pixel-radius measurements determined directly from the images in each frame, ranging from ~ 0.25 magnitudes for the WF chips to ~ 0.65 magnitudes for the PC. Based on our simulations, the use of mean aperture corrections applied to all clusters in a given WF chip is likely to introduce a random error of ≈ 0.1 magnitudes to the photometry of any individual cluster. To convert to B and I magnitudes we used the gain ratios and zeropoints given by Holtzman et al. (1995; 1997). The final magnitudes and colors of all detected objects are plotted in Figure 3, and are available in electronic form from CJG.

Completeness tests were carried out by adding a total of ≈ 3000 artificial stars to each image and processing the results in a manner identical to that used for the original data. Artificial globulars (generated from a composite PSF derived from real images in each frame) were added in batches of 100 with successively fainter B magnitudes, and with colors $B - I = 0.3, 1.3$, and

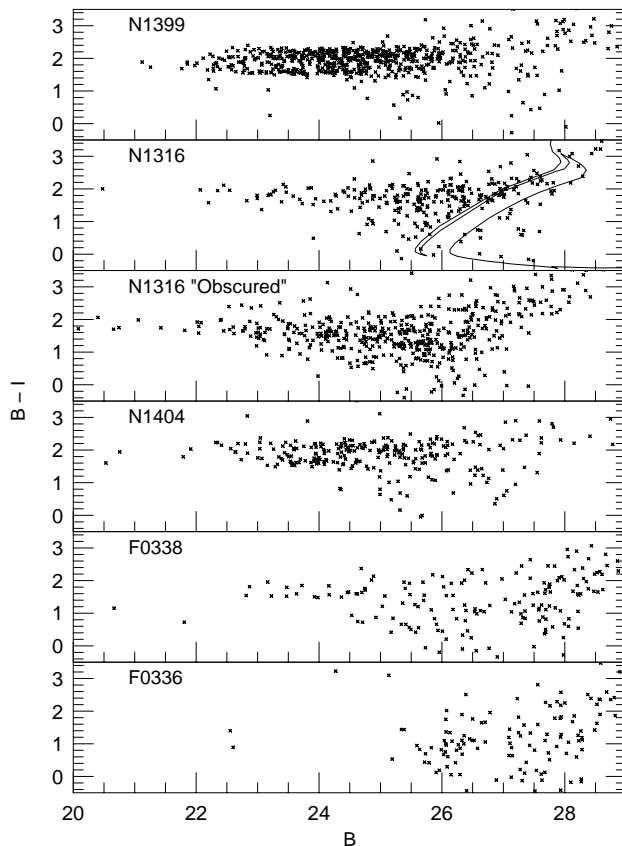


Fig. 3.— Colors and magnitudes for all compact sources in the WFPC2 frames. An electronic tabulation of the photometry is available on request from CJG. The solid line in the NGC 1316 panel shows the color-magnitude sequence (subgiant and horizontal branch) expected for a stellar population of age 4×10^7 yrs and $[\text{Fe}/\text{H}] = -0.4$.

2.3 magnitudes, respectively. The results of these tests are shown for NGC 1399 in Figure 4 and Figure 5. The 50% completeness level for the bulk of the detected objects occurs at $B \approx 26.8$ in the WF frames, and ≈ 25.8 in the PC images. For F0336, the 50% completeness level for the same color occurs at $B \approx 27.3$ in the WF frames, and $B \approx 26.9$ in the PC. The completeness tests for NGC 1399 yield an estimate for the photometric uncertainty for $1.3 < B - I < 2.3$ of ≈ 0.08 mag rms at $B = 25$, and ≈ 0.17 mag rms at $B = 26$.

3. The Color Distributions.

In Figure 6 we show the numbers of globular clusters found per 0.1 mag color interval brighter than $B = 26.0$ in each of the five fields. The corresponding surface densities for the three galaxies are tabulated in Table 2. The shaded regions in Figure 6 show the color distributions for objects brighter than $B = 25.0$. Assuming that the color distribution of any intergalactic globular clusters roaming

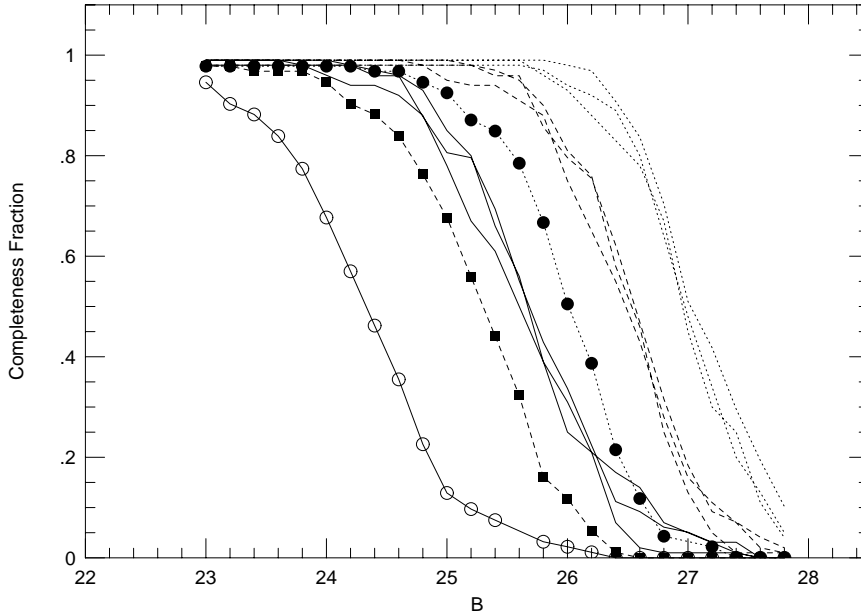


Fig. 4.— Completeness fraction as a function of B magnitude for NGC 1399. Solid lines show the results for $B - I = 0.3$, dashed lines correspond to $B - I = 1.3$, and dotted lines to $B - I = 2.3$. Lines with symbols show the results for the PC, while all others indicate completeness fractions for the WF chips.

the Fornax cluster should be similar to that seen in the three galaxies in our sample, the distribution apparent in F0336 indicates that such clusters are rare, and that the apparent distribution of colors is primarily representative of unresolved background galaxies. Completeness fractions were computed by spline-interpolation of our color-magnitude completeness grid. Correcting each bin by simply dividing by the computed completeness fraction and subtracting the F0336 distribution yields the distributions indicated by the dotted lines in Figure 6.

The color distributions of globular clusters in both NGC 1399 and NGC 1404 are evidently bimodal. Moreover, the colors of the peaks and the overall width of the color distributions are almost identical, though NGC 1399 may have a slightly larger proportion of red clusters. The mean $B - I$ colors of the two samples are 2.01 ± 0.46 and 1.98 ± 0.58 , and a Kolmogorov-Smirnov test indicates that the hypothesis that the two populations were drawn from the same parent population cannot be rejected at the 63% confidence level. Based on the ratios of the numbers of globular clusters counted to $B = 25$ and $B = 26$, it appears that the bluer clusters are on average somewhat brighter than the red clusters. We discuss this finding further in Section 4 and in Forbes et al. (1998).

The higher surface density of globular clusters around NGC 1404, as well as the difference in mean colors when compared with a similar field on the opposite side of NGC 1399 (F0338),

Table 2. Fornax Globular Cluster Color Distribution

$B - I$	NGC 1399		NGC 1404			NGC 1316	
	N	f^a (arcmin ⁻²)	N	f^a (arcmin ⁻²)	f^b (arcmin ⁻²)	N	f^a (arcmin ⁻²)
-0.1– 0.0	0	0.0	2	0.4	0.1	1	3.8
0.0– 0.1	1	0.0	0	0.0	0.0	1	0.6
0.1– 0.2	1	-0.2	1	-0.2	0.2	1	0.3
0.2– 0.3	1	0.2	0	0.0	0.0	1	1.7
0.3– 0.4	0	0.0	0	0.0	0.0	0	0.0
0.4– 0.5	0	-0.4	1	-0.2	-0.4	2	0.8
0.5– 0.6	1	0.0	1	0.0	-0.4	2	1.4
0.6– 0.7	0	-0.2	2	0.3	-0.1	3	1.5
0.7– 0.8	2	0.5	1	0.2	-0.4	1	0.6
0.8– 0.9	3	-0.1	2	-0.5	-0.2	4	1.7
0.9– 1.0	1	0.0	0	-0.2	-0.2	6	3.0
1.0– 1.1	3	0.7	4	1.0	1.0	4	2.2
1.1– 1.2	0	0.0	3	0.7	0.3	2	1.0
1.2– 1.3	1	0.2	0	0.0	-0.6	4	2.1
1.3– 1.4	4	0.7	2	0.2	0.0	10	4.3
1.4– 1.5	15	2.8	7	0.9	1.1	7	2.7
1.5– 1.6	46	9.7	14	2.7	0.6	11	4.8
1.6– 1.7	50	10.8	24	5.1	4.5	18	8.0
1.7– 1.8	46	10.4	23	4.8	4.1	21	9.2
1.8– 1.9	48	10.2	17	3.6	3.0	17	7.5
1.9– 2.0	59	12.6	21	4.1	3.6	16	6.6
2.0– 2.1	88	18.7	29	6.1	5.9	12	5.1
2.1– 2.2	67	14.2	26	5.5	5.1	7	3.1
2.2– 2.3	70	14.7	16	3.4	3.4	1	0.4
2.3– 2.4	19	4.0	8	1.7	1.5	1	0.4
2.4– 2.5	3	0.6	2	0.4	0.4	1	0.4
2.5– 2.6	2	0.5	0	0.0	0.0	0	0.0
2.6– 2.7	2	0.4	0	0.0	0.0	0	0.0
2.7– 2.8	0	0.0	0	0.0	0.0	0	0.0

Note. —

^aSurface density after completeness correction and subtraction of the background as determined from F0336.

^bSurface density after completeness correction and subtraction of the color distribution in F0338, which lies on the opposite side of NGC 1399 at a distance similar to that of NGC 1404.

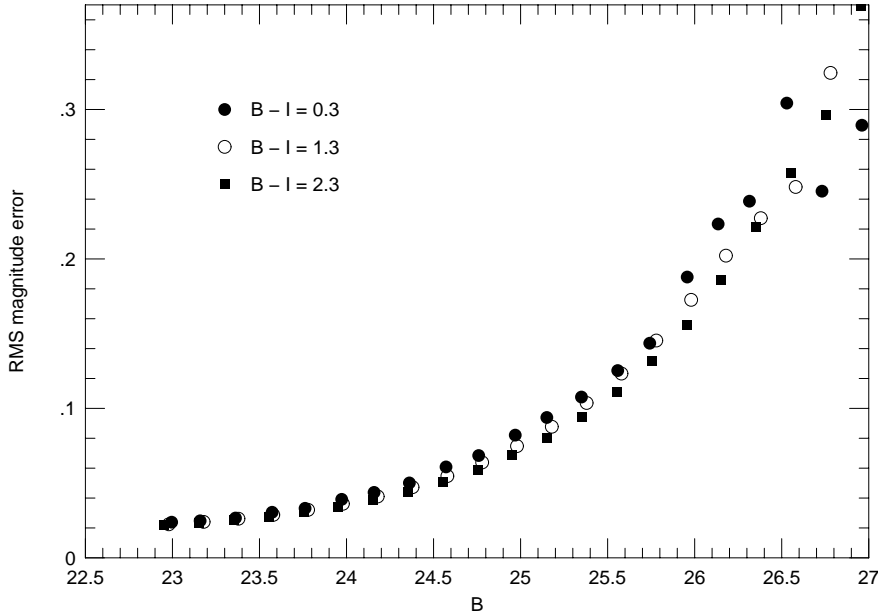


Fig. 5.— Estimates of the RMS uncertainties in magnitudes for clusters in NGC 1399, as derived from a comparison of the input magnitudes of model clusters and the magnitudes returned after processing.

indicate that these globular clusters indeed belong to NGC 1404 as opposed to the much more populous and extended population of NGC 1399. Taking into account the orientations and the area-weighted centers of the WFPC2 field-of-view in NGC 1404 and F0338, we find that the F0338 field is $0.39'$ closer in projection to NGC 1399 than the NGC 1404 field. Assuming a radial surface density profile of NGC 1399 globular clusters which goes as $f \propto r^{-1.5}$ (e.g. Kissler-Patig et al. 1997a), we apply a correction factor of 0.93 to the surface density of globulars detected in F0338 to match the surface density of NGC 1399 globulars expected at the radius of NGC 1404. Subtracting the resulting, completeness-corrected distribution of globular clusters in F0338 from that of NGC 1404 yields the dotted line in Figure 6. The total number of globular clusters and the mean color are minimally affected, supporting the notion that the majority of these globular clusters are indigenous to NGC 1404. Furthermore, the similarity in the color distributions of NGC 1399 and NGC 1404 are consistent with the idea that NGC 1399’s overabundance of globular clusters may have come partly at the expense of NGC 1404 and other galaxies in the Fornax cluster (Forbes et al. 1997b; Kissler-Patig et al. 1998). This does not, of course, rule out the possibility that the red and blue clusters originated in different galaxies or under different circumstances.

Interestingly, the color distribution of compact sources in F0338 appears to be significantly different from those seen in the galaxy-centered fields. Even after subtraction of the color distribution in F0336 (the background field), the colors of objects in F0338 peak at $B - I = 0.6$, which is 0.1 magnitudes bluer than the centroid of the bluest peak in either NGC 1399 or NGC 1404. There

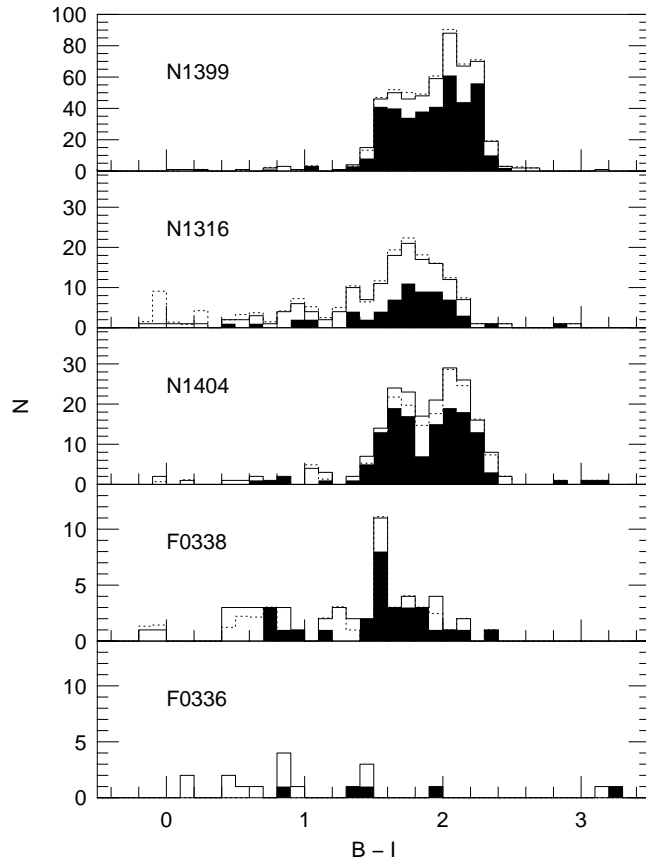


Fig. 6.— Color distribution of compact sources in the five Fornax fields. The shaded regions indicate the numbers of objects with $B < 25.0$, while the solid lines indicate the numbers of objects with $B < 26.0$. The dotted lines correspond to the completeness-corrected and background-subtracted counts. The dotted line shown for NGC 1404 shows the effect of background-subtraction using the color distribution observed in the F0338 field and thereby better characterizes the color distribution of globular clusters native to NGC 1404.

is also a group of objects with $B - I < 1$ which appears to significantly exceed the number of such objects found in the F0336. These findings are consistent with the presence of a significant color gradient, as first reported by Ostrov et al. (1993). These observations and their consequences are discussed in detail by Forbes et al. (1998).

In spite of the possibility of unseen, distributed dust, the “unobscured” objects in NGC 1316 are on average 0.45 magnitudes bluer in $B - I$ than either those in NGC 1399 or NGC 1404. The peak in the number counts occurs just redward of the position of the bluest peak in NGC 1399 and NGC 1404, with a significant tail of objects with $B - I < 1.2$. The bluer objects are much less luminous than the bright, blue clusters found by Holtzman et al. (1992) in NGC 1275. The lack of bright, blue globulars, while perhaps surprising given the ample evidence for a recent merger event, agrees with the findings of Shaya et al. (1996). However, this may not be entirely surprising given the much smaller quantity of dust visible in NGC 1316 than in NGC 1275. And despite the

arguments of Shaya et al. (1996), we cannot rule out bright young clusters in the obscured, highly reddened central regions of the galaxy. Very young ($\tau \sim 5$ Myrs) *stellar* populations do produce stars as bright as $M_B = -9$. However, such stars would mostly be far hotter and bluer than the objects we detect in NGC 1316. Shown in Figure 3 is the $B - I$ color-magnitude sequence of the turnoff and horizontal branch expected for a stellar population of age 4×10^7 yrs and $[\text{Fe}/\text{H}] = -0.4$ (Worthey, private communication). While bearing a general resemblance to the distribution of the faintest objects in NGC 1316, the luminosity function for such a stellar population requires a very much larger number of hot, blue objects ($B - I < 0.5$) than we actually find.

Many of the objects surrounding NGC 1316 are similar in color and magnitude to the old open clusters or the faint, metal-poor, outlying globular clusters in our own Galaxy such as PAL 1 and Eridanus. Based on the models of Worthey (1994), the objects with $25 < B < 26$ and $1.2 < B - I < 2.2$ are consistent with a population of old, metal-poor clusters with masses of order $10^5 M_\odot$, or metal-rich clusters with ages as young as 1 Gyr and masses of order $10^4 M_\odot$. We discuss the nature of these objects further in Section 5.

Both Whitmore et al. (1995) and Elson & Santiago (1996a, 1996b) used *HST* data to confirm the presence of color dichotomies in the GC system of M 87 first suggested by the ground-based data of Lee & Geisler (1993). The color differences between the blue and red peaks in the color histograms of globular clusters in M 87 are $\Delta(V - I)_0 \approx 0.25$ magnitudes. However, the $B - I$ color is about twice as sensitive to metallicity as $V - I$. If we assume that age is not an important contributor to the spread in color, and if we use Couture, Harris, & Allwright’s (1990) color-metallicity calibrations for Milky Way globular clusters, we find that the full-width-at-half-maxima for the color distributions of Elson & Santiago (1996) and Whitmore et al. (1995) ($\Delta(V - I)_0 \approx 0.45$ mag) correspond to a spread in $[\text{Fe}/\text{H}]$ of about 2.3 dex. NGC 1399 and NGC 1404 have $\Delta(B - I)_0 \approx 0.8$ in both NGC 1399 and NGC 1404, yielding a metallicity spread $\Delta [\text{Fe}/\text{H}] \approx 2.1$ dex. These values are in good agreement with the metallicity spread inferred from $C - T_1$ measurements of the brighter globulars in NGC 1399 by Ostrov et al. (1993). Using only the color differences between peaks in M 87, NGC 1399, and NGC 1404, we find $\Delta [\text{Fe}/\text{H}] \approx 1.3, 1.1,$ and 1.1 dex, respectively. As found in previous ground-based studies (see Geisler et al. 1996 for a tabulation), the ranges of globular cluster metallicities to be found in M 87 and NGC 1399 (and other bright ellipticals) are similar, spanning an interval which extends from the metal-poorest globulars in our Galaxy to a metallicity significantly higher than that of the sun.

4. The Luminosity Functions.

The luminosity functions (LFs) for our three target galaxies are given in Table 3 and are plotted in Figures 7 and 8. The plotted LFs for NGC 1399 and NGC 1316 have been corrected for completeness, and background-corrected by subtracting the observed, completeness-corrected LF of F0336. Similarly, the GCLF for NGC 1404 has been adjusted using the completeness-corrected (but not background subtracted) LF in F0338 after scaling by a factor of 0.93 as described earlier to account for the fact that the center of the F0338 field is 0'.4 closer to NGC 1399 than is NGC 1404. Completeness corrections were made for each globular cluster counted based on the WFPC2 chip on which it was found, but no account was taken of the cluster's position on the chip.

The LF for objects in NGC 1316 is clearly different from those of NGC 1399 and NGC 1404. In addition to a bluer mean color, the number of objects in NGC 1316 increases rapidly faintwards and does not show a log-normal distribution of the kind normally seen in globular cluster systems. We discuss NGC 1316's cluster system in more detail below.

The GCLFs for NGC 1399 and NGC 1404 appear to be very similar. A straightforward comparison using the Kolmogorov-Smirnov test reveals that the null hypothesis (that the two populations were drawn from the same parent population) cannot be rejected at the 90% confidence level. If the magnitudes of NGC 1404 globular clusters are offset by $B = -0.27$ magnitudes (see below), the K-S test yields a probability of 74% in favor of the null hypothesis. After binning, completeness correction, and background subtraction, a χ^2 test over the range $20 < B < 26.5$ gives an 86% probability in favor of the null hypothesis.

We have used version 2.0 of the peak-finding code described by Secker & Harris (1993) (and kindly provided by J. Secker) to compute the maximum-likelihood peaks and dispersions of both Gaussian and Student's t_5 functions from our GCLF sample. Owing to the current limitations of the code we have used only the globular clusters detected in the WF frames, for which the completeness functions are reasonably similar. As we are neglecting only 10% (20%) of the total number of clusters detected around NGC 1399 (NGC 1404), the statistics are not seriously affected. For the present purposes we use only clusters with colors in the range $1.2 < B - I < 2.6$. The results are given in Table 4. We also include maximum-likelihood fits to the Milky Way and M 31 cluster data described below, and we quote the values given by Whitmore et al. (1995) for the *HST* V-band data of M 87. We assume reddenings of $E(B-V) = 0.11$ and 0.01 for M 31 and Fornax, respectively (Burstein & Heiles 1982; Schlegel, Finkbeiner, & Davis 1998). Figure 9 shows the χ^2 contours for the NGC 1399 B-band GCLF Gaussian fit in the peak-dispersion plane. For each entry in Table 4 the listed uncertainties correspond to the projections of the 1σ contours onto the peak magnitude and dispersion axes. The Gaussian which best fits the combined NGC 1399 + NGC 1404 data is shown in Figure 10. The value of $\langle m_V^0 \rangle = 23.73 \pm 0.06$ we find for NGC 1399 is in good agreement with the value of $\langle m_V^0 \rangle = 23.77 \pm 0.06$ (after extinction correction using our adopted reddening) determined by Kohle et al. (1996) from ground-based data.

Table 3. Fornax Globular Cluster Luminosity Functions

B	NGC 1399		NGC 1404		NGC 1316	
	N	f^a (arcmin $^{-2}$)	N	f (arcmin $^{-2}$)	N	f (arcmin $^{-2}$)
20.1–20.3	0	0.0	0	0.0	0	0.0
20.3–20.5	0	0.0	0	0.0	1	0.4
20.5–20.7	0	0.0	1	0.0	0	0.0
20.7–20.9	0	0.0	1	0.2	0	0.0
20.9–21.1	0	0.0	0	0.0	0	0.0
21.1–21.3	2	0.4	0	0.0	0	0.0
21.3–21.5	0	0.0	0	0.0	0	0.0
21.5–21.7	0	0.0	0	0.0	0	0.0
21.7–21.9	3	0.6	1	0.0	0	0.0
21.9–22.1	2	0.4	1	0.2	1	0.4
22.1–22.3	8	1.7	0	0.0	1	0.4
22.3–22.5	10	1.9	3	0.6	2	0.6
22.5–22.7	15	2.5	4	0.4	1	-0.2
22.7–22.9	14	2.9	4	0.8	2	0.8
22.9–23.1	15	3.2	5	0.7	3	1.3
23.1–23.3	25	5.3	4	0.4	5	2.1
23.3–23.5	26	5.5	8	1.3	4	1.7
23.5–23.7	28	5.9	15	2.9	2	0.8
23.7–23.9	29	6.1	6	0.9	3	1.3
23.9–24.1	33	6.7	22	4.2	4	1.5
24.1–24.3	46	9.7	6	1.1	4	1.7
24.3–24.5	41	8.7	22	3.5	5	2.1
24.5–24.7	39	8.3	16	2.0	9	3.8
24.7–24.9	35	7.2	8	0.7	14	5.9
24.9–25.1	35	7.5	18	3.5	8	3.5
25.1–25.3	39	7.8	15	1.9	18	7.5
25.3–25.5	30	6.4	16	2.3	17	8.2
25.5–25.7	28	7.4	14	3.8	25	11.8
25.7–25.9	24	4.5	15	3.7	22	13.9
25.9–26.1	20	4.0	13	1.3	15	6.1
26.1–26.3	17	1.6	6	0.1	21	8.2
26.3–26.5	19	3.9	5	-2.0	19	14.5

Note. —

^aSurface density after background subtraction and completeness correction.

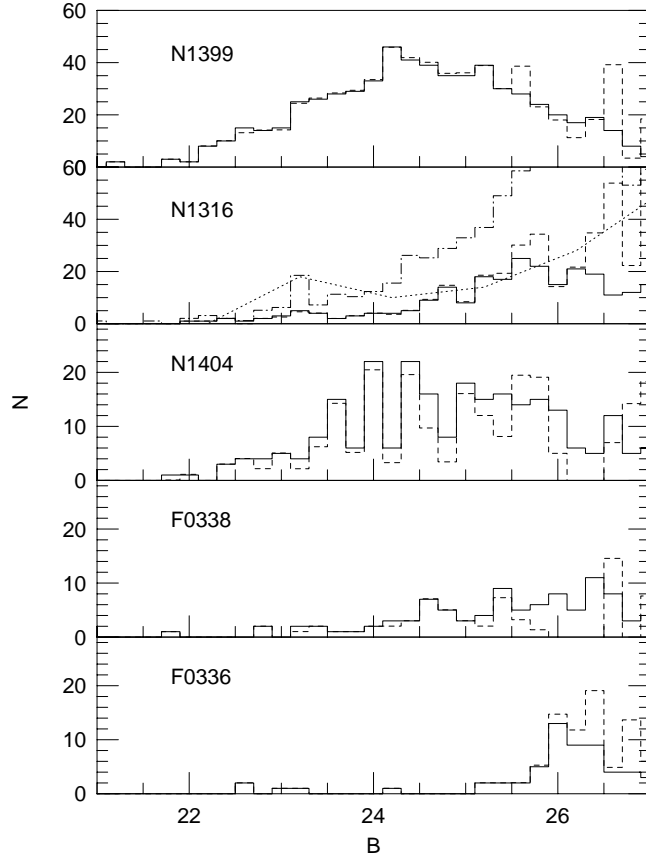


Fig. 7.— Luminosity functions of point sources in the five Fornax fields. For NGC 1399, NGC 1316, and F0338, the dashed lines show the effects of dividing by the computed completeness fractions and subtracting the completeness-corrected luminosity function observed in field F0336. For NGC 1404, the dashed curve shows the effect of subtracting the F0338 luminosity function from observed distribution in NGC 1404. The dashed line in the F0336 panel simply shows the effect of dividing by the computed completeness fractions. The dash-dot lines for NGC 1316 shows the effect of including those objects detected in the obscured regions in the WF chips. The dotted curve for NGC 1316 shows the “completeness-corrected” luminosity function of Galactic open clusters tabulated by van den Bergh & Lafontaine (1984), multiplied by a factor of 10.

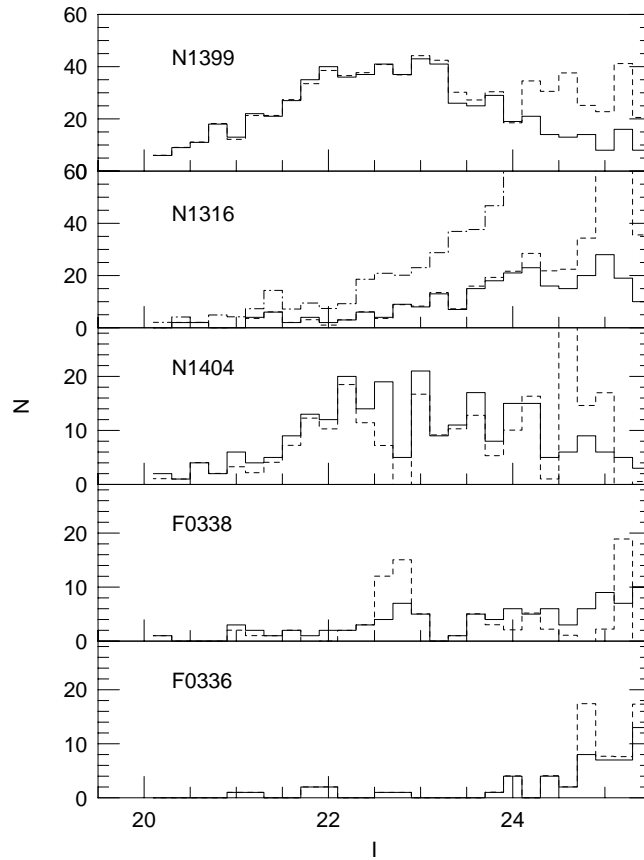


Fig. 8.— *I*-band luminosity functions of point sources in the five Fornax fields. The dashed lines are as described in Figure 7.

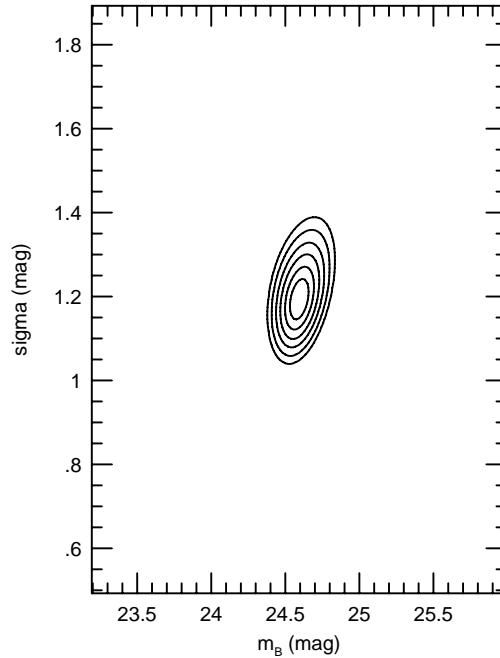


Fig. 9.— Contours of χ^2 in the $\langle m_V^0 \rangle$ - σ plane for the combined luminosity functions of NGC 1399 and NGC 1404, using the method of Secker & Harris (1993). The contours range from 0.5σ to 3σ and are spaced at intervals of 0.5σ .

The peak magnitudes computed for NGC 1399 and NGC 1404 differ by 0.27 ± 0.22 magnitudes in the sense that NGC 1404 may lie some 2.1 Mpc beyond NGC 1399, though the uncertainty is large. The GCLF width for NGC 1404 is evidently slightly broader than that for NGC 1399, though again the uncertainties on the NGC 1404 result do not rule out identical widths.

As this is the first time we have been able to examine the LF of Fornax globular clusters to this depth, it is interesting to compare it with the LFs of Local Group globular clusters. In Figure 10 we compare the background-corrected, combined GCLF for NGC 1399 and NGC 1404 (after shifting the latter by -0.27 magnitudes) to the LFs of globular clusters in our own Galaxy and M 31. The Milky Way GCLF derives from the halo globular cluster compilation of Harris (1996) on the McMaster University WWW page². The data for globular clusters in M 31 comes from the halo sample tabulated by Reed et al. (1994), and we assume $(m-M)_0 = 24.43$ for M 31 (Ajhar et al. 1995). The Local Group GCLFs are compared with the completeness- and background-corrected GCLF of NGC 1399 + NGC 1404, shifted assumed $(m-M)_0 = 31.05$ (see below) and $E(B - V) = 0.01$ (Schlegel, Finkbeiner, & Davis 1998). The Local Group GCLFs have been normalized to the total number of GCs counted in NGC 1399 and NGC 1404 with $M_B < -5$.

While the Milky Way GCLF appears in most respects to be fairly similar in form to the GCLF for NGC 1399 + 1404, the GCLF for M 31 globular clusters appears to be somewhat more peaked.

²<http://www.physics.mcmaster.ca/Globular.html>

Table 4. Parametric Fits to Globular Cluster Luminosity Functions

	$\langle m_B^0 \rangle$ (Gaussian)	σ	$\langle m_B^0 \rangle$ (t_5)	σ	$\langle m_V^0 \rangle$ (Gaussian)	σ
Milky Way	-6.49 ± 0.19	1.54 ± 0.15	-6.61 ± 0.17	1.28 ± 0.15		
M 31	17.38 ± 0.11	1.05 ± 0.08	17.41 ± 0.11	0.90 ± 0.09		
NGC 1399	24.55 ± 0.08	1.19 ± 0.05	24.56 ± 0.08	1.07 ± 0.06	23.73 ± 0.08	1.19 ± 0.05
NGC 1404	24.82 ± 0.20	1.41 ± 0.15	24.84 ± 0.21	1.20 ± 0.15		
NGC 1399 ($B - I > 1.9$)	24.71 ± 0.08	1.16 ± 0.06	24.70 ± 0.08	1.05 ± 0.07		
NGC 1399 ($B - I < 1.9$)	24.32 ± 0.12	1.24 ± 0.09	24.34 ± 0.09	1.10 ± 0.08		
NGC 1399 + NGC 1404	24.62 ± 0.07	1.23 ± 0.05	24.62 ± 0.08	1.09 ± 0.05	23.77 ± 0.06	1.22 ± 0.05
M 87 ^a					23.72 ± 0.06	1.40 ± 0.06

Note. —

^aValues quoted from Whitmore et al. 1995.

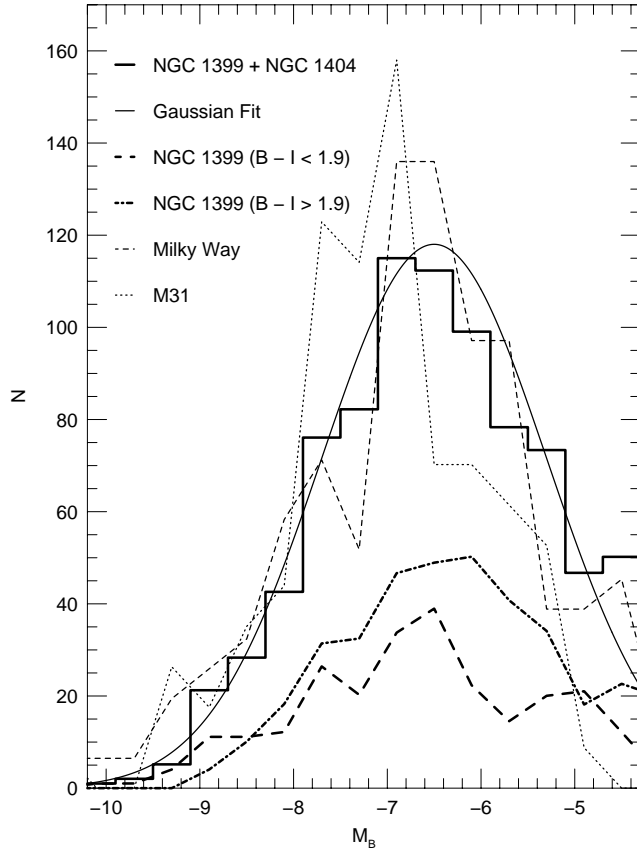


Fig. 10.— Luminosity functions of NGC 1399 and NGC 1404 compared with the luminosity functions for halo globulars in the Galaxy and M 31. The Local Group luminosity functions have been normalized to the same total number of globulars as found in the combined NGC 1399 and NGC 1404 samples. Also shown are separate luminosity functions for the blue and red globulars in NGC 1399. The Gaussian fit results from the application of version 2 of Secker & Harris’s (1993) maximum-likelihood estimator. The difference between the apparent peak in the uncorrected data and that of the Gaussian are due to incompleteness and photometric errors, which are properly handled by the program.

The computed GCLF widths determined for the Galaxy and M 31 are broader and narrower, respectively, than we find for the early-type galaxies. The uncertainty on the GCLF width of Galactic globulars is large enough to accommodate the Fornax and M 87 results, but the M 31 distribution is clearly at odds with all others. The mean magnitudes and widths we find for the M 31 GCLF are consistent with those determined for the outer-halo M 31 globulars by Kavelaars & Hanes (1997). Incompleteness of the M 31 sample at the faint end, though difficult to quantify, must be at least partially responsible for this discrepancy. In any event, the numbers of Local Group globular clusters are too small to allow strong conclusions to be made. A χ^2 test comparing the NGC 1399 + 1404 GCLF with the Milky Way and M 31 GCLFs indicates that the null hypothesis remains valid at the 66% and 63% confidence levels, respectively. Similarly comparing the NGC 1399 + 1404 GCLF with the combined Milky Way and M 31 GCLFs yields a probability for the

null hypothesis of greater than 64%.

Ashman, Conti, & Zepf (1995) have shown that good agreement between the measured GCLF peaks of early-type and late-type galaxies could be achieved by accounting for the different opacities and increased line-blanketing expected in higher metallicity systems. For NGC 1399 in particular, they predict an offset $\Delta\langle m_B^0 \rangle = 0.26$ mag with respect to the peak observed in the Milky Way. Using this offset and the values in Table 4, we find $(m - M)_0 = 30.78 \pm 0.21$. Ashman et al.’s (1995) models were computed using only Gaussian dispersions. However, since their model distributions were symmetric, the $\Delta\langle m_B^0 \rangle$ for t_5 distribution should be very similar. The peak magnitudes computed for the Milky Way and NGC 1399 using the t_5 function then yield $(m - M)_0 = 30.91 \pm 0.19$. The agreement between these distance moduli and those determined using other distance-measuring techniques (see below) underscores the remarkable uniformity in the underlying mass functions of globular clusters in very different galaxy types.

Also shown in Figure 10 are the LFs for the 230 bluer ($B - I < 1.9$) and the 348 redder ($B - I > 1.9$) globular clusters in NGC 1399. According to Table 4 there is no significant difference between the widths of these two distributions, and it appears from Figure 10 that a simple faintward shift of the blue distribution could bring it into line with the red one. This is reflected in the mean and peak magnitudes in Table 4, which differ by 0.36 ± 0.12 mags (t_5) between the red and blue samples. After shifting the red LF by -0.36 magnitudes, a χ^2 test gives a probability for the null hypothesis of 51%. Current data for two positions in M 87 (Whitmore et al. 1995; Elson & Santiago 1996b) and NGC 5846 (Forbes et al. 1997a) are consistent with the blue peak being from 0.0 to 0.3 magnitudes brighter in V than the red peak. If attributed entirely to metallicity effects, the 0.36 B -band magnitude difference we find for NGC 1399 clusters would correspond to $\Delta[Fe/H] \approx 1$ dex (Couture et al. 1990), and would produce a V -band difference between the two peaks of ≈ 0.2 magnitudes.

In Figure 11 we compare the GCLF for NGC 1399 with the V -band, *HST* GCLF for M 87 of Whitmore et al. (1995). We have converted our B -band measurements to V -band for the comparison using

$$(B - V)_0 = 0.347(B - I)_0 + 0.163, \quad (1)$$

which is a least-squares fit to the least-reddened ($E(B-V) < 0.4$) Galactic globular clusters as compiled on the McMaster WWW page. Simply comparing values of $\langle m_V^0 \rangle$ in Table 4 reveals that the peak of the NGC 1399 GCLF is 0.01 ± 0.10 magnitudes fainter than that of M 87. This is in good agreement with offsets of 0.05 ± 0.09 magnitudes found by Kohle et al. (1996) and 0.08 ± 0.16 magnitudes found by Blakeslee & Tonry (1996) from deep, ground-based GCLF studies, after correction for our adopted reddening. The NGC 1399 GCLF was recomputed after applying a shift of -0.01 to the computed V magnitudes to bring the peak into line with that of M 87 as per Table 4. The resulting V -band luminosity function is compared with a scaled version of Whitmore et al.’s (1995) M 87 GCLF in the upper panel of Figure 11.

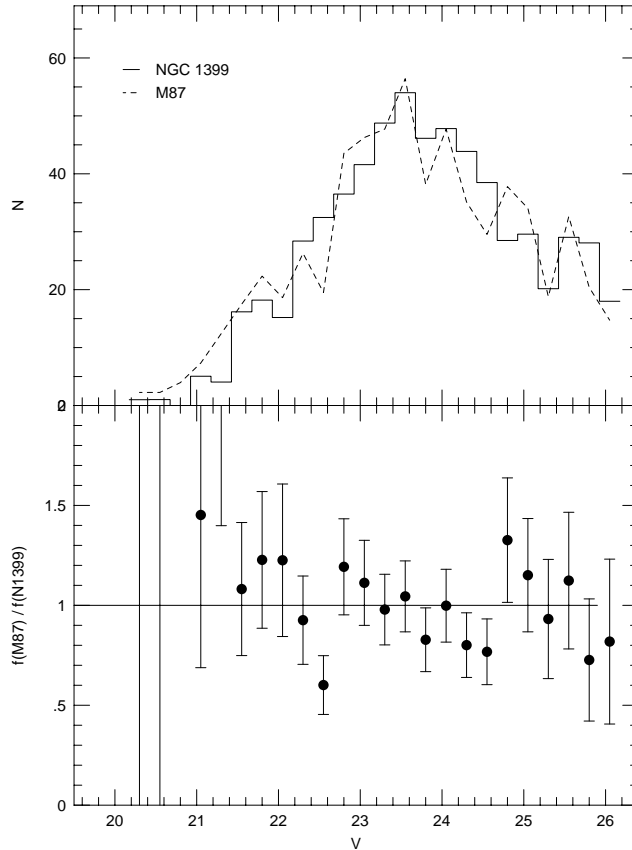


Fig. 11.— The globular cluster luminosity function of NGC 1399, after conversion to V -band magnitudes (as described in the text) and shifting by -0.1 mag, compared with the HST GCLF determined by Whitmore et al. (1995) for M 87. The lower panel shows the bin-by-bin ratio of the M 87 GCLF to the normalized GCLF of NGC 1399. The error bars reflect Poisson statistics only.

There is clearly very little difference between the GCLFs of the two cD galaxies. In the lower panel of Figure 11 we show the bin-by-bin ratio of the normalized M 87 luminosity function to that of NGC 1399. The GCLFs are evidently indistinguishable over most of the range of comparison, though there may be proportionately more very bright globulars in M 87 than there are in NGC 1399. A χ^2 test indicates that the null hypothesis cannot be rejected at the 69% confidence level.

The GCLF width listed in Table 4 for NGC 1399 is significantly narrower ($\approx 4\sigma$) than that found by Whitmore et al. 1995 for M 87. This is due in part to the very bright M 87 globulars noted above, and in part to differences in the methods used to measure the widths; the method of Secker & Harris (1993) we have adopted here takes into account the broadening of the LF due to photometric errors. The GCLF width we find for NGC 1399 is very similar to those found for NGC 4278, NGC 4494 (Forbes 1996b) and NGC 1404, but is significantly narrower than those of either NGC 4365 GCLF (Forbes 1996a) or NGC 5846 (Forbes et al. 1996), all measured using the

code of Secker & Harris (1993). Thus, NGC 1399 does not support Kissler-Patig et al.’s (1997a) suggestion that GCLF properties vary little among the lesser galaxies, be they early or late-type, but that they vary significantly among cluster-dominating ellipticals.

Adopting for M 87 a distance of 16.1 ± 1.3 Mpc (Ferrarese et al. 1997; Yasuda et al. 1997), then the relative shift of 0.01 ± 0.1 magnitudes we find for the GCLF of NGC 1399 gives a distance to Fornax of 16.2 ± 1.5 Mpc. This is in good agreement with a Fornax distance of 16.9 ± 1.1 Mpc determined by McMillan, Ciardullo, & Jacoby (1993) using planetary nebula luminosity functions, though in somewhat poorer agreement with the distance of 18.4 ± 1.8 Mpc determined by Madore et al. (1996) using *HST* observations of Cepheids in NGC 1365. While Cepheids are believed to be more accurate distance indicators than GCLFs, it may also be that NGC 1365 lies well out at the periphery of the Fornax cluster, as spiral galaxies are wont to do. Since NGC 1399 sits almost exactly at the center of the cluster’s potential well, we can use our inferred distance to compute a value for the Hubble constant without incurring the additional uncertainty introduced by the expanse of the Fornax cluster itself. We use a heliocentric velocity for Fornax of 1450 ± 34 km s⁻¹ (Held & Mould 1994). Correcting for the solar motion with respect to the Local Group (-91 km s⁻¹; Yahil, Tammann, & Sandage 1977), and a Virgocentric infall component along the line of sight to Fornax of 36 km s⁻¹ (Tammann & Sandage 1985), we obtain an expansion-induced velocity of 1323 ± 34 km s⁻¹. This then yields a Hubble constant $H_0 = 82 \pm 8$ km s⁻¹ Mpc⁻¹, where the uncertainty reflects random measurement errors only. This agrees reasonably well with a value of 73 ± 6 (random) ± 8 (systematic) km s⁻¹ Mpc⁻¹ found by Madore et al. (1996) using, among other things, *HST*-measured Cepheid distances to several nearby galaxy groups including Virgo and Fornax.

5. The Case of NGC 1316

Why is the LF of clusters in NGC 1316 not log-normal in form, as are those of almost all globular cluster systems studied to date? One might postulate that the LF of objects surrounding NGC 1316 reflects a young system which has yet to undergo depletion by the disruption of its faintest members. Removal of the majority of objects fainter than $B \approx 24.5$ could conceivably leave behind a log-normal LF. However, the number of objects at $B = 24.5$ is small, and such a depletion would leave NGC 1316 with roughly as many clusters as NGC 1404. The specific frequency of globular clusters in NGC 1404 is already quite low ($S_N \sim 2$, Forbes et al. 1997), and given the 1.4 magnitude difference in total luminosity between these two galaxies, we would be left with a remarkably low $S_N \approx 0.5$ for NGC 1316. While this would be highly unusual for any early-type galaxy, it would be even more surprising in view of NGC 1316’s evident merger history and apparent dominance of its corner of the Fornax cluster.

If NGC 1316 has undergone a significant starburst and is destined to fade by at least a factor of four in the time required to disrupt the fainter clusters, it is conceivable that S_N might eventually approach a value more typical of early-type galaxies. However, a direct comparison between the WF3 images of NGC 1316 and NGC 1404 reveals that the ratio in the total luminosities of these two galaxies is largely preserved in surface brightness measurements at the larger radii where NGC 1316 appears to be free of dust. It seems unlikely that significant recent star formation has taken place at these large radii, and that we must therefore be looking primarily at old stars. Thus, even if there is substantial fading of a younger stellar population residing at the center of NGC 1316, the total magnitude (and therefore S_N) will be largely unaffected.

The luminosity function of the objects we see in NGC 1316 has been seen in other galaxies as well, NGC 4038/4039 (Whitmore & Schweizer 1995) and NGC 3597 (Carlson et al. 1998) being two well-studied cases. Superposed on the NGC 1316 luminosity function in Figure 7 is the “completeness-corrected” luminosity function of Galactic open clusters tabulated by van den Bergh & LaFontaine (1984), scaled upwards by a factor of 10. While there may be relatively fewer bright objects in NGC 1316 than there are open clusters in the Galaxy, the luminosity functions are reasonably similar over the range for which we have good statistics.

In Figure 12 we show the distribution of clusters over $m_1 - m_2$ (the difference between magnitudes measured for one- and two-pixel-radius apertures) and magnitude for NGC 1316’s unobscured clusters and for NGC 1399 globular clusters which fall in the same, outer portions of the WFPC2 detectors. (By limiting our comparison to the same regions of the detectors we minimize the effects that position-dependent changes in the shape of the PSF might have on object centering.) The mean measured $m_1 - m_2$ for objects with $I < 25$ are identical, but the overall distribution of $m_1 - m_2$ is about 40% broader for NGC 1316 than it is for NGC 1399. Whereas a Kolmogorov-Smirnov test shows that the distributions of $m_1 - m_2$ of clusters in NGC 1399 and NGC 1404 cannot be distinguished at the 50% confidence level, comparing NGC 1399 and NGC 1316 using the same test indicates that we can reject the null hypothesis at $> 99.8\%$ confidence level.

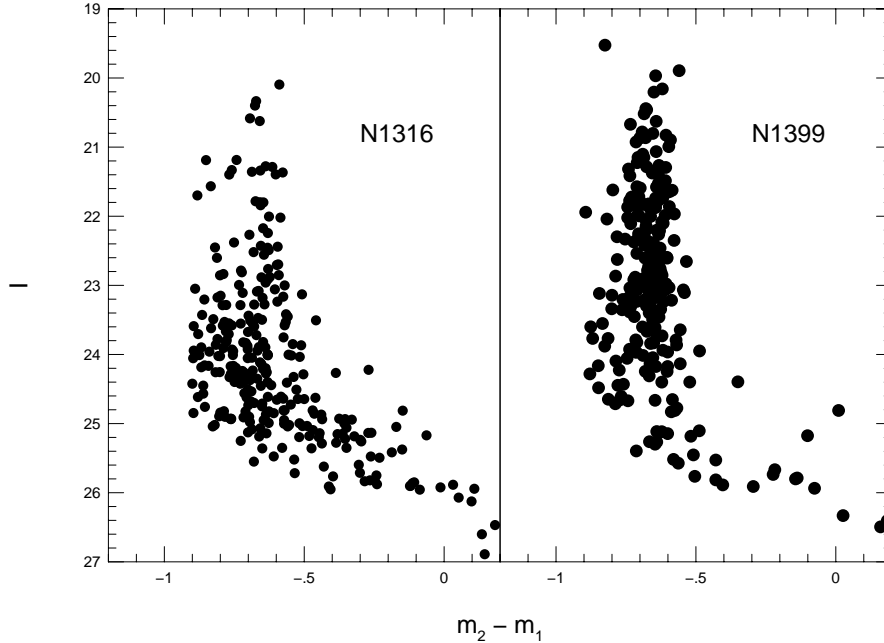


Fig. 12.— The distribution of $m_2 - m_1$, the difference in magnitude between apertures of radius one pixel and apertures of radius two pixels, as measured in the F814W frames. The clusters in NGC 1399 have been sampled from the same portions of the CCD frames used for the unobscured clusters in NGC 1316. Note that a cutoff of $m_2 - m_1 = -0.9$ (-1.1 for the PC frames) has already been imposed to excise as many background galaxies from the sample as possible.

The distribution of colors, magnitudes, and $m_1 - m_2$ in NGC 1316 is in some respects similar to that of compact field objects in F0336, but the total surface density of objects is some 15 times larger. Disregarding the possibility that there may be an undiscovered, populous cluster of galaxies situated beyond NGC 1316 which mimics the color and luminosity distribution of field galaxies, it is exceedingly unlikely that the observed number of objects in NGC 1316 could be a chance fluctuation in the density of background galaxies. Moreover, over the limited, dust-free region available in the WFPC2 field of view, the radial distribution of the unobscured clusters with $B < 26.5$ follows a powerlaw form with $\alpha \approx -1.5 \pm 0.5$. This is not significantly different from NGC 1316’s surface brightness profile, which Shaya et al. (1996) found to have an asymptotic slope of -1.16 ± 0.02 . This is consistent with the radial distributions of many other cluster systems and supports our view that these objects must be physically associated with NGC 1316.

Given the recent merger which has clearly taken place in NGC 1316, one might have expected significant numbers of metal-rich *globular* clusters to have formed as prescribed by the model of Ashman & Zepf (1992). However, neither we nor Shaya et al. (1996) (who also studied objects in the dust-obscured central regions) have found evidence for presumed young globular clusters of the type found by Holtzman et al. (1992) in NGC 1275 and Whitmore et al. (1993) in NGC 7252. This may be due to the much smaller amount of gas and dust in NGC 1316 compared to

these other galaxies. Alternatively, perhaps the active nucleus and twin jets of NGC 1316 are preventing the condensation of gas clouds sufficiently large to produce globular clusters. Inspection of the Northeastern quadrant of NGC 1316 in Figure 2 reveals structures in the dust which are reminiscent of the photoevaporating columns of M 16 (Hester et al. 1996), though on a much larger scale. The radially-oriented columns in the dust could be a result of erosion by a radiation or particle flux originating in the central regions of the galaxy. Alternatively, we may be seeing Rayleigh-Taylor instabilities in action. NICMOS observations of the tips of these columns may be useful in determining whether proto-open clusters are indeed condensing out of the material.

Given that the only large open cluster populations we know of are in spiral galaxies, would the existence of large numbers of open clusters in NGC 1316 imply that the merger remnant we see today must at one time have been a sizable spiral? This would certainly be consistent with the presence of dust, though the relatively small amount of dust compared with the amount seen in NGC 1275 suggests that NGC 1316’s intruder may have been a smaller or an earlier type of spiral. Could it be that many early-type galaxies have exponential cluster luminosity functions (or at least significant exponential components), but that they have only really become detectable with the advent of the *HST*? If the objects in NGC 1316 really are old open clusters, where are the globular clusters? If NGC 1316 had itself also been a spiral galaxy before the merger, then a globular cluster specific frequency of ~ 0.5 might not seem so unreasonable. However, a merger between two spiral galaxies generating virtually no new globular clusters would be at odds with the model predictions of Ashman & Zepf (1992). Could it be that the clusters we see in NGC 1316 started out as all cluster systems do, but that they have somehow avoided the tidal shocking and disruption which may be responsible for the log-normal GCLF seen in most other galaxies (Vesperini 1998)? Given the anomaly that NGC 1316’s cluster system represents, these questions are well worth pursuing and may provide us with an important key to understanding both star cluster and galaxy formation.

6. Intergalactic Globular Clusters.

Theuns & Warren (1996), Arnaboldi et al. (1996), and Ferguson et al. (1997) recently detected significant numbers of stars and planetary nebulae at rather large distances from the cD galaxies NGC 1399 and M 87. Grillmair et al. (1994a) found that globular clusters around NGC 1399 seem to be kinematically related more to the whole Fornax cluster than to the central galaxy itself. This has prompted us to examine our data for evidence of such intergalactic nomads among the globular clusters in our sample. The various components of the Fornax cluster (stars, globular clusters, and cluster galaxies) all seem to fall off with distance from NGC 1399 as $f \propto r^{-1.5}$ (e.g. Grillmair et al. 1994a; Kissler-Patig et al. 1997a). In the WF frames only, we find 517, 74, and 48 objects with $B < 26.5$ in fields N1399, F0338, and F0336, respectively.

The radial surface density distributions of globular clusters in cD galaxies generally have a fairly extended “core” (Grillmair et al. 1986; Lauer & Kormendy 1986; Grillmair et al. 1994b)

where the surface density becomes nearly constant. If we thus ignore our central pointing and assume that in the outer parts the surface density falls off as r^α , then solving

$$f = ar^\alpha + b \tag{2}$$

for $\alpha = -1.5$ and using only the outer fields at 0.14 and 1.4 degrees, we find $b = 10.4 \pm 1.5 \text{ arcmin}^{-2}$. Thus the surface density of unresolved objects (10.6 arcmin^{-2}) at 1.4 from NGC 1399 would be entirely consistent with a roughly constant surface density of compact background galaxies. Put another way, under the assumption that the globular cluster surface density profile maintains a power-law form with $\alpha = -1.5$ at all radii, we would predict only 0.8 ± 0.3 globular clusters in our outermost field. [As an aside, this powerlaw would predict 750 ± 170 globular clusters in our NGC 1399 field, or about 60% more than we actually see, which is consistent with the degree of core-flattening in the surface density distribution found by Kissler-Patig et al. (1997a)]. If we adopt the flatter slope with $\alpha = -1.2$ found by Forbes et al. (1998), we would predict 1.7 ± 0.7 globular clusters in our outermost field. Clearly, the data are consistent with no intergalactic globular clusters at 1.4 , but are insufficient to rule them out.

Despite the relatively large color/metallicity spread in NGC 1399’s globular cluster system, Figure 3 demonstrates how well defined their distribution is over color and magnitude compared to the background field. Indeed, one could draw a box with $22 < B < 27$ and $1.5 < B - I < 2.3$ and capture more than 95% of the cluster sample. If we then place such a box over the color-magnitude distribution of objects in F0336, we find a total of 7 objects crowding the very faint end of the box. Close visual inspection of these objects reveals that two of the seven objects are probably galaxies, but we cannot rule out that the remaining five objects may be globular clusters in the envelope of NGC 1399. However, if this is so, then the color-magnitude distribution of these outlying clusters must be very different from those near the center of the galaxy; the odds of obtaining the observed color-magnitude distribution by sampling the GCLF in Figure 7 are vanishingly small.

7. Summary and Conclusions.

We have analyzed WFPC2 images of three early-type galaxies and two background fields in the Fornax cluster. From an investigation of the global distribution over color and magnitude, we conclude the following:

- The color distributions of globular clusters in the central regions of NGC 1399 and its nearby neighbor NGC 1404 are bimodal, and statistically very similar to one another.
- With respect to the color distributions seen in NGC 1399 and NGC 1404, objects in a field $8.5'$ from NGC 1399 have a significant blueward bias. The metallicity gradient found by Ostrov et al. (1993) in NGC 1399 appears to be present even among the faintest clusters.

- The luminosity functions of globular clusters in NGC 1399 and NGC 1404 are essentially identical to one another and very similar to the luminosity function of globulars in M 87.
- The luminosity function for the blue globulars in NGC 1399 peaks 0.36 ± 0.12 magnitudes brighter in B than the luminosity function of the red clusters.
- The luminosity function of objects surrounding NGC 1316 is unlike that found for globular clusters in the other galaxies. Based on the bluer color distribution, the exponential shape of the luminosity function, and the relatively large spread in cluster sizes, we tentatively identify these objects with an extensive population of old *open* clusters.
- The measured peak of NGC 1399’s luminosity function (converted to V -band magnitudes) is 0.01 ± 0.1 magnitudes fainter than that of M 87, yielding $H_0 = 82 \pm 8 \text{ km s}^{-1} \text{ Mpc}^{-1}$, where the uncertainty reflects only the effects of random errors.
- We see no evidence for intergalactic globular clusters, though our field of view is too small to strongly constrain this finding.

CJG is grateful to S. Faber and J. Kormendy for many interesting and useful discussions. We also thank M. Kissler-Patig for a critical reading of the manuscript. Finally, we are grateful to an anonymous referee for a very helpful report. This research was supported in part by STScI Grant No. GO-05990.01-94A, and by faculty research funds from the University of California, Santa Cruz.

REFERENCES

- Ajhar, E. A., Grillmair, C. J., Lauer, T. R., Baum, W. A., Faber, S. M., Holtzman, J. A., Lynds, C. R., & O’Neil, E. Jr. 1996, *AJ*, 111, 1110
- Ashman, K. M., & Zepf, S. E. 1992, *ApJ*, 384, 50
- Ashman, K. M., Conti, A., & Zepf, S. E. 1995, *AJ*, 110, 1164
- Ashman, K. M., & Zepf, S. E. 1997, *Globular Cluster Systems*, Cambridge University Press, in press.
- Baum, W. A., Hammergren, M., Groth, E. J., Ajhar, E. A., Lauer, T. R., O’Neil Jr., E. J., Lynds, C. R., Faber, S. M., Grillmair, C. J., Holtzman, J. A. & Light, R. M. 1995, *AJ*, 110, 2537
- Blakeslee, J. P., & Tonry, J. L. 1996, *ApJ*, 465, L19
- Bridges, T. J., Hanes, D. A., & Harris, W. E. 1991, *AJ*, 101, 469
- Brodie, J. P. 1981, PhD Thesis, University of Cambridge.
- Burstein, D., & Heiles, C. 1982, *AJ*, 87, 1165
- Carlson, M. et al. 1998, in preparation.
- Couture, J., Harris, W. E., & Allwright, J. W. B. 1990, *ApJS*, 73, 671
- Dawe, J. A., & Dickens, R. J. 1976, *Nature*, 263, 395
- Elson, R., & Santiago, B. X. 1996a, *MNRAS*, 278, 617
- Elson, R., & Santiago, B. X. 1996b, *MNRAS*, 280, 971
- Elson, R., Grillmair, C. J., Forbes, D. A., Rabban, M., Williger, G. M., & Brodie, J. P. 1998, */mnras*, 295, 240
- Ferrarese, L. et al. 1997, *ApJ*, 475, 853
- Forbes, D. A. 1996a, *AJ*, 112, 954
- Forbes, D. A. 1996b, *AJ*, 112, 1409
- Forbes, D. A., Brodie, J. P., & Huchra, J. 1996, *AJ*, 112, 2448
- Forbes, D. A., Brodie, J. P., & Huchra, J. 1997a, *AJ*, 113, 887
- Forbes, D. A., Brodie, J. P., & Grillmair, C. J. 1997b, *AJ*, 113, 1652
- Forbes, D. A., Grillmair, Williger, G. M., C. J., Elson, R., & Brodie, J. P. 1998, *MNRAS*, 293, 325
- Geisler, D., & Forte, J. C. 1990, *ApJ*, 350, L5
- Geisler, D., Lee, M. G., & Kim, E. 1996, *AJ*, 111, 1529
- Grillmair, C.J., Pritchett, C., & van den Bergh, S. 1986, *AJ*, 91, 1328
- Grillmair, C. J., Freeman, K. C., Bicknell, G. V., Carter, D., Couch, W., Sommer-Larsen, J., & Taylor, K. 1994a, *ApJ*, 422, L9

- Grillmair, C.J., Faber, S.M., Lauer, T.R., Baum, W.A., Lynds, C.R., O’Neil, E.J. Jr., & Shaya, E.J. 1994b, AJ, 108, 102
- Grillmair, C. J., Forbes, D. A., & Elson, R. E. 1997, in preparation.
- Hanes, D. A., & Harris, W. E. 1986, ApJ, 309, 564
- Harris, W. E., & Hanes, D. A. 1987, AJ, 93, 1368
- Harris, W. E., Allwright, J. W. B., Pritchett, C. J., & van den Bergh, S. 1991, ApJS, 76, 115
- Harris, W. E. 1996, AJ, 112, 1487
- Held, V., & Mould, J. R. 1994, AJ, 107, 1307
- Hester, J. et al. 1996, AJ, 111, 2349
- Holtzman, J. A., 1997, private communication.
- Holtzman, J. A., Faber, S. M., Shaya, E. J., Lauer, T. R., Groth, E. J., Hunter, D. A., Baum, W. A., Ewald, S. P., Hester, J. F., Light, R. M., Lynds, C. R., O’Neil, E. J. Jr., Westphal, J. A. 1992, AJ, 103, 691
- Holtzman, J. A., Burrows, C. J., Casertano, S., Hester, J. J., Trauger, J. T., Watson, A. M., & Worthey, G. 1995, PASP, 107, 1065
- Holtzman, J. A. et al. 1996, AJ, 112, 416
- Kavelaars, J. J., & Hanes, D. A. 1997, MNRAS, 285, 31
- King, I. R. 1966, AJ, 71, 64
- Kissler-Patig, M., Kohle, S., Hilker, M., Richtler, T., Infante, L., & Quintana, H. 1997a, A&A, 319, 470
- Kissler-Patig, M., Brodie, J. M., Schroder, L., Forbes, D. A., Grillmair, C. J., & Huchra, J. 1997b, submitted.
- Kissler-Patig, M., Grillmair, C. J., Meylan, G., Brodie, J. P., Minniti, D., & Goudfrooij, P. 1998, submitted.
- Kohle, S., Kissler-Patig, M., Hilker, M., Richtler, T., Infante, L., & Quintana, H., 1996, A&A, 309, 39
- Krist, J. 1995, in *Astronomical Data Analysis Software and Systems IV*, ASP Conference Series, 77, p 349.
- Lauer, T., & Kormendy, J. 1986, ApJ, 303, L1
- Lee, M. G., & Geisler, D. 1993, AJ, 106, 493
- Madore, B. F. et al. 1996, BAAS, 189, 108.04
- McMillan, R., Ciardullo, R., & Jacoby, G. H. 1993, ApJ, 416, 62
- Ostrov, P., Geisler, D., & Forte, J.C. 1993, AJ, 105, 1762
- Reed, L. G., Harris, G. L. H., & Harris, W. E. 1994, AJ, 107, 555

- Richtler, T., Gerbel, E. K., Domgorgen, H., Hilker, M., Kissler, M. 1992, *A&A*, 264, 25
- Schlegel, D. J., Finkbeiner, D. P., & Davis, M. *ApJ*, 500, 525
- Secker, J., & Harris, W. E. 1993, *AJ*, 105, 1358
- Shaya, E. J., Dowling, D. M., Currie, D. G., Faber, S. M., Ajhar, E. A., Lauer, T. R., Groth, E. J., & Grillmair, C. J. 1996, *AJ*, 111, 2212
- Stetson, P. 1987, *PASP*, 99, 191
- Stetson, P. B. 1994, *PASP*, 106, 250
- Schweizer, F. 1980, *ApJ*, 237, 303
- Tammann, G. A., & Sandage, A. 1985, *ApJ*, 294, 81
- van den Bergh, S., & Lafontaine, A. 1984, *AJ*, 89, 1822
- Vesperini, E. 1998, *MNRAS*, in press.
- Wagner, S., Richtler, T., & Hopp, U. 1991, *A&A*, 241 399
- Whitmore, B. C., Schweizer, F., Leitherer, C., Borne, K., & Robert, C. 1993, *AJ*, 106, 1354
- Whitmore, B. C., & Schweizer, F. 1995, *AJ*, 109, 960
- Whitmore, B. C., Sparks, W. B., Lucas, R. A., Macchetto, F. D., Biretta, J. A. 1995, *ApJ*, 454, L73
- Yahil, A., Tammann, G. A., & Sandage, A. 1977, *ApJ*, 217, 903
- Yasuda, N., Fukugita, M., & Okamura, S. 1997, *ApJS*, 108, 417
- Zepf, S. E., & Ashman, K. M. 1993, *MNRAS*, 264, 611

This figure "fig1.jpg" is available in "jpg" format from:

<http://arxiv.org/ps/astro-ph/9809210v1>

This figure "fig2.jpg" is available in "jpg" format from:

<http://arxiv.org/ps/astro-ph/9809210v1>